Gauss map and Lyapunov exponents of interacting particles in a billiard

Cesar Manchein and Marcus W. Beims [*]

*Departamento de Física, Universidade Federal do Paraná,
81531-990 Curitiba, PR, Brazil*

Abstract

We show that the Lyapunov exponent (LE) of periodic orbits with Lebesgue measure zero from the Gauss map can be used to determine the main qualitative behavior of the LE of a Hamiltonian system. The Hamiltonian system is a one-dimensional box with two particles interacting via a Yukawa potential and does not possess Kolmogorov-Arnold-Moser (KAM) curves. In our case the Gauss map is applied to the mass ratio ($\gamma = m_2/m_1$) between particles. Besides the main qualitative behavior, some unexpected peaks in the γ dependence of the mean LE and the appearance of 'stickness' in phase space can also be understand via LE from the Gauss map. This shows a nice example of the relation between the "instability" of the continued fraction representation of a number with the stability of non-periodic curves (no KAM curves) from the physical model. Our results also confirm the intuition that pseudo-integrable systems with more complicated invariant surfaces of the flow (higher genus) should be more unstable under perturbation.

Key words: Lyapunov exponents, Gauss map, Continued fraction, Billiard

1 Introduction

The Gauss map [1,2,3] is a chaotic map which generates the integers from a simple Continued Fraction (CF) representation of a real number. CFs have been used in several different scientific context like, for example, the renormalization group theory [4,5,6], expansion technique applied to a model for Bloch electrons in a magnetic field [7], stability of elementary particles [8] and their mass ratio representation [8,9]. In the context of nonlinear dynamics it has

---

[*] Corresponding author
Email address: `mbeims@fisica.ufpr.br` (Marcus W. Beims).

been applied to compute stable and unstable directions of maps [10], to approximate irrational winding numbers for the KAM tori [11] and to determine critical parameter values at which the KAM tori break [12,13,14].

In this paper we discuss the stability of perturbed tori in a different situation. The unperturbed system is the problem of two particles in a 1D-Box interacting via Hard Point-like Collisions (HPC). Depending on the mass ratio between particles, the system can be integrable (Invariant Surface (IS) of the flow is a torus with genus $g = 1$), pseudo-integrable (IS has a more complicated topology with $g > 1$) and ergodic (see [15,16,17]). Since the HPC case is linearly unstable, the LE is zero for each mass ratio and little is known about the stability of the IS. Since the Hamiltonian is not differentiable at the boundary and at the collisions, no KAM curves exist for any perturbation. Classical [15] (quantum [15,16]) results strongly suggest that the classical dynamics (level statistics) is more unstable (Gaussian Orthogonal Ensemble (GOE) distribution) for the pseudo-integrable than the integrable cases. Here the perturbed system is obtained by changing the HPC to a Yukawa interaction (YI). Recent classical results [18] also suggest that pseudo-integrable IS from the HPC are more unstable than the integrable ones when the YI is turned on. We show here that the chaotic dynamics in the perturbed system, the 1D-Box with YI, is directly related with the chaotic property of the *number* related to the mass ratio $\gamma = m_2/m_1$ between particles. To do this we compare the LE from the infinite continued fraction representation of γ with the maximal LE from the two interacting particles in the 1D box. In fact, we show that the qualitative behavior of the LE in the YI case can be reproduced qualitatively using the LE from the Lebesgue Measure (LM) zero Periodic Orbits from Gauss Map (POGM). We also show that the dynamics in the Yukawa case is more unstable when POGM are closer to non-POGM. In these cases 'stickiness' (tendency of orbits to get trapped) appears more often in phase space. This is shown by using the most probable Lyapunov exponent, proposed recently [18] as a very sensitive tool to probe globally details in phase space dynamics.

It is well known from the KAM theorem that in two-dimensional systems the torus surface does not exist if $\alpha = \omega_1/\omega_2$ lies in a region for rational numbers, where w_1, w_2 are the frequencies of the unperturbed problem. The region for rational numbers increases as the perturbation parameter increases. Therefore, only those irrationals that are hardest to approximate by rationals will yield the KAM surface. The residue criterion [13] establishes a correspondence between the existence of a KAM curve and the stability of the periodic orbits that approximate it. In other words, the stability of *periodic orbits* very close to *non-periodic orbits* (KAM curves), allows to make some statements about the destruction of the KAM curve. In our case the situation is different, the LE calculated for the *periodic orbits* with LM zero from the Gauss map, i. .e. the *non-periodic curves* from the physical model (not KAM curves), allows us to get some insight about the stability of the IS from a linear unstable

system with LE zero. Therefore we have a *direct relation between the invariant surfaces with zero LEs and their stability under perturbation.*

In section 2 the main results from the 1D-Box HPC are summarized. Section 3 analyzes those properties of the Gauss map which are relevant for the purpose of this paper. We calculate explicitly the LE for the POGM with LM zero which differ from the ergodic result. Section 4 introduces the smooth Yukawa interaction between particles and the LE distribution is calculated. The relation between the mean LE from the physical model and the LE from the POGM is demonstrated. The paper ends with conclusions in section 5.

2 Two particles in a 1D-Box with hard point-like collisions

Two particles in a 1D-box with HPC can be treated as a particular case of the motion of three particles on a finite ring [19,20], which can be mapped onto the motion of a particle in a triangle billiard [21]. The whole dynamics can be monitorated by changing the angles of the triangle billiard. These angles are functions of the masses ratio between particles. It is possible to show [22] that the dynamics is non-ergodic if θ is a rational multiple of π, where

$$\cos(\theta) = \frac{1 - m_2/m_1}{1 + m_2/m_1} = \frac{1 - \gamma}{1 + \gamma}. \tag{1}$$

Writing $\theta = \frac{m}{n}\pi$, where m and n are integers, at most $4n$ distinct velocity values occur. These are the periodic orbits from the problem. Although there are infinite mass ratios which give rational values of θ/π, some of them are special: the integrable cases [23] $\gamma = 1, 3$ (or $1/3$), which have $\theta = \frac{1}{2}\pi$ and $\theta = \frac{2}{3}\pi$ (or $\pi/3$), respectively. These are the cases for which the genus $g = 1$ [24] (the IS of the billiard flow is a torus). For all other rational θ/π the dynamics is pseudo-integrable [20], the invariant flow is not a torus and gets more and more complicated as g increases ($1 < g < \infty$) [17]. It was shown [16] that for small g the spectral statistics is close to semi-Poisson and it approaches the GOE statistics when g is increased. Table 1 shows some rational angles for the right triangle billiards with $g \leq 3$ and their relation with the mass ratio γ and θ/π obtained from Eq. (1). For genus $g = 2$, for example, the values of θ are: $\frac{1}{4}\pi, \frac{1}{5}\pi$ and the mass ratio are respectively $\gamma \sim 0.17$ and $\gamma \sim 0.11$. On the other hand, when θ is an irrational multiple of π, the velocities become uniformly dense [25] in velocity space. As a consequence, it is at least *possible* for the two-particle with HPC to be ergodic in velocity space.

Since the 1D-Box HPC is linear unstable [26], all LEs are zero and little is known about the stability of the above mentioned ISs. In this work we propose to analyse the stability of the 1D-Box HPC using results from the Gauss map.

genus (g)	p/q	θ/π	γ	$1/\gamma$	$\lambda^G(x_{k,800})$	$x_{k,800}$(CF)
1	1/4	1/2	1	1	7.37	$[\overline{2,800}] \sim 1/2$
Integrable	1/6	1/3	1/3	3	7.78	$[\overline{3,800}] \sim 1/3$
2	1/8	1/4	0.17	5.89	8.07	$[\overline{4,800}] \sim 1/4$
Pseudo-Int.	1/10	1/5	0.11	9.47	8.30	$[\overline{5,800}] \sim 1/5$
3	1/12	1/6	0.07	13.9	8.47	$[\overline{6,800}] \sim 1/6$
Pseudo-Int.	1/14	1/7	0.05	19.2	8.64	$[\overline{7,800}] \sim 1/7$

Table 1

Some rational angles p/q (see [16]) for genus $g \leq 3$ from the triangle billiards and their relation with the mass ratio γ and θ/π obtained from Eq. (1). $\lambda^G(x_{k,800})$ is the LE obtained from period-2 orbits of the Gauss map calculated very close (on the left) to θ/π. The last row shows the CF representation of the $x_{k,800}$ used to calculate the LE.

We will show that, associating the irrational values of θ/π (and therefore γ) with properties of the LE for the LM zero POGM, we are able to make some statements about the stability of the ISs with LE *zero* from the HPC case.

3 The Gauss map

In this section the main properties of the Gauss map will be reviewed and some numerical calculations for the LE will be performed. For more details we refer to the works of Corless et al [2,3] and references therein. The Gauss map for x in the interval $(0,1)$ is given by

$$G(x) = \frac{1}{x} - \left[\frac{1}{x}\right]. \tag{2}$$

The notation [.] means to take the fractional part. The LE exponent can be calculated from

$$\lambda^G(x) = \lim_{j \to \infty} \frac{1}{j} ln \left(\prod_{i=1}^{j} |G'(x_i)| \right), \tag{3}$$

whenever this limit exists, where $G'(x_i) = \partial G(x_i)/\partial x_i$. The Gauss map generates the numbers $n_1, n_2, n_3, \ldots$ from the simple CF representation of a real number

$$x = n_0 + \cfrac{1}{n_1 + \cfrac{1}{n_2 + \cfrac{1}{n_3 + \cdots}}}, \tag{4}$$

where the n_i are all positive integers, except n_0 which may be zero or negative. Here we consider $n_0 = 0$. The CF is represented in the form $x = n_0 + [n_1, n_2, n_3, \ldots]$. For rational values of x the sequence of n_i is finite and the LE from Eq. 3 cannot be calculated. For irrational x the sequence is infinite. For irrational quadratic values of x, the sequence of n_i are periodic, as exemplified below. The Gauss map is ergodic and for almost all initial conditions the LE may be calculated explicitly by $\lambda^G(x) = \pi^2/6 \log 2 = 2.3731\ldots$. *Periodic orbits* in the Gauss map occur when a sequence of integers repeat. A fixed point has the property $x_{n_1} = [n_1, n_1, n_1, \ldots]$, which is written in a more simplified manner as $[\overline{n}_1]$. For period-1 periodic orbits the LE can also be calculated explicitly, however it is *different* from the almost-everywhere values (in the Lebesgue sense). It can be calculated from $\lambda^G(x_{n_1}) = 2ln(1/x_{n_1})$. For the golden-mean number $x = (\sqrt{5} - 1)/2$, for example, we have $n_1 = 1$ and $\lambda^G(x_1) = 2ln(1/x_{n_1}) = 0.96\ldots$ which is the lowest LE. All initial conditions in $(0, 1)$ which have the property $x = [n_1, n_2, n_3, \ldots, n_k, 1, 1, 1, \ldots]$, have the LE equal to ~ 0.96. Period-2 orbits have the form $x = [n_1, n_2, n_1, n_2 \ldots] = [\overline{n_1, n_2}]$, period-3 orbits have $x = [\overline{n_1, n_2, n_3}]$, and so on. Note that for any rational x the limit $j \to \infty$ from Eq.(3) does not exist and the LE cannot be determined.

Now we give a numerical summary of the above results for the LE of period-1 and period-2 orbits in the Gauss map. If we iterate the Gauss map many times $(j \to \infty)$ using arbitrary initial conditions between the interval $(0, 1)$, all orbits have LEs equal to ~ 2.3731, which is calculated using Eq. (3). This is the ergodic result and it is shown by the solid line in Fig. 1. Note that in this numerical procedure, due to numerical errors it is impossible to get exactly the POGM when $j \to \infty$. As a consequence the LE is always ~ 2.3731. However, for *low* period-p orbits we can calculate the LE which *differs* from this ergodic results, since just few iterations are needed and numerical errors do not have time to propagate. We use the following procedure, we chose a period-p POGM map, determine the corresponding initial value of x and then calculate numerically the corresponding LE $\lambda^G(x)$ using $j = p$. For period-1 orbits we have for $n_1 = 1, 2, 3, 4$:

$$x_1 = 0.618033989\ldots = [1, 1, 1, \ldots] = [\overline{1}], \qquad \lambda^G(x_1) \sim 0.96,$$

$$x_2 = 0.414213562\ldots = [2, 2, 2, \ldots] = [\overline{2}], \qquad \lambda^G(x_2) \sim 1.76,$$

$$x_3 = 0.302775638\ldots = [3, 3, 3, \ldots] = [\overline{3}], \qquad \lambda^G(x_3) \sim 2.38,$$

$$x_4 = 0.236067977\ldots = [4, 4, 4, \ldots] = [\overline{4}], \qquad \lambda^G(x_4) \sim 2.88.$$
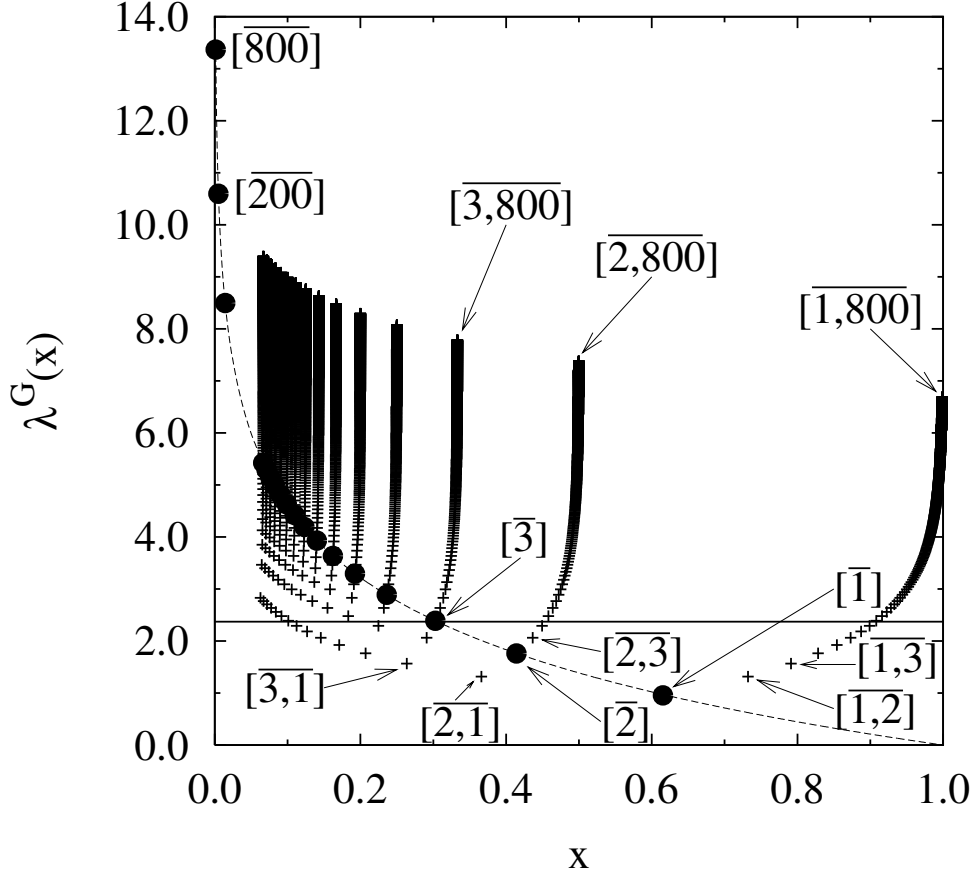
Fig. 1. Lyapunov exponents for period-1 and period-2 orbits from the Gauss map in the interval $(0, 1)$.

We observe that using these value of x_k $(k = 1, 2, 3, 4)$, after one iteration of the Gauss map the LEs differ from the ergodic result. The LEs $\lambda^G(x_k)$ for period-1 points are plotted as circles in Fig. 1. They are exactly on the dashed line, which is the curve $\ln G'(x)$ for just one iteration. Points along the dashed line are the LE $\lambda^G(x)$ from the Gauss map only when $x = x_1, x_2, \ldots$. Later we will explain the reason why we plotted the dashed line.

We can also calculate the LE for period-2 orbits. Some explicit example are

$$x_{2,1} = 0.366025\ldots \sim \overline{[2, 1]}, \qquad \lambda^G(x) \sim 1.32,$$

$$x_{3,1} = 0.263762\ldots \sim \overline{[3, 1]}, \qquad \lambda^G(x) \sim 1.56,$$

$$x_{4,1} = 0.207106\ldots \sim \overline{[4, 1]}, \qquad \lambda^G(x) \sim 1.76.$$

We generated the values of $x = \overline{[n_1, n_2]}$ for Period-2 orbits using all combinations of n_1, n_2. These points are marked as crossed points in Fig. 1,

6

where some corresponding CF representations are shown. Different sequences (branches) of x values are observed. Sequences start (from below) at $[\overline{1}]$, $[\overline{2,1}]$, $[\overline{3,1}], \ldots [\overline{k,1}] \ldots, [\overline{800,1}]$. We could increase the last value of k but it is not relevant for the discussion here. In all simulations the last k used was $k = 800$. In Fig. 1 we showed only the 15 first sequences, they come closer and closer as k increases. Inside each sequence the CF representation changes its second number. For example, the first sequence, on the right, starts at the Golden mean $[\overline{1}]$ with the lowest LE for this sequence and the LE increases with period-2 orbits $[\overline{1,2}]$, $[\overline{1,3}]$ until $[\overline{1,800}]$, which has a LE ~ 6.69. The next sequence of period-2 orbits is $[\overline{2,1}]$, $[\overline{2,2}]$, $[\overline{2,3}], \ldots, [\overline{2,800}]$. The last point from this sequence has a LE equal ~ 7.37. In fact, for $x_{2,k=\infty} = [\overline{2,\infty}]$, which is exactly equal $1/2$, the limit of (3) does not exist and the LE cannot be calculated. Using the periodic orbit $x_{2,800} = [\overline{2,800}] \sim 1/2$ we are allowed to calculate the LE $\lambda^G(x_{2,800}) \sim 7.37$ very close (on the left) to the non-periodic orbit $x = 1/2$.

The next sequence (see Fig. 1) starts at $[\overline{3,1}]$ and ends at $x = [\overline{3,800}] \sim 1/3$ with LE ~ 7.78. The subsequent sequences converge to $[\overline{4,800}] \sim 1/4$ with $\lambda^G(x_{4,800}) \sim 8.07$, $[\overline{5,800}] \sim 1/5$ with $\lambda^G(x_{5,800}) \sim 8.30 \ldots$, $[\overline{800,800}] \sim 0.0012$ with $\lambda^G(x_{800,800}) \sim 13.4$. It is important to observe that the LE increases more and more as k increases. For all these points the LE calculated for the POGM *differ* from the ergodic result ~ 2.3731. While such POGM have LM zero and may not be relevant for the Gauss map itself, we will show they contribution in a physical problem. We just need to relate the Gauss map and the 1D-Box HPC from section 2 through $x = \theta/\pi$.

4 Yukawa interaction, results and discussion

In order to study the stability of the ISs from the HPC case, we need to apply a perturbation on the system. Therefore, we assume now that the interaction between particles is given by the Yukawa potential

$$V(r) = V_0 \frac{e^{-\alpha r}}{r}, \tag{5}$$

which has strength V_0 and the parameter $\alpha \geq 0$ gives the interaction range $r_0 = 1/\alpha$. The classical dynamics of this problem was already analyse for equal masses [27] and for mass ratios γ in the interval $(1, 4)$ [18].

Using the above interaction, we calculated the finite-time maximal LE as a function of the mass ratio in the interval $(0, 4)$. Results are shown in Fig. 2(a) for the distribution $P(\Lambda_t, \gamma)$ of the finite-time largest Lyapunov exponents [28] Λ_t and Fig. 2(b) for the mean $\langle \Lambda_t \rangle$ (see solid line). The mean LE decreases

from roughly 1.18 for $\gamma \sim 0.0$ to 0.59 for $\gamma = 4.0$. An unexpected pronounced peak is observed at $\gamma \sim 1.0$. When the value of γ decreases, the mean LE exponent presents a minimum at $\gamma \sim 0.85$ and then increases again until another unexpected lower peak close to $\gamma \sim 0.11$ [better seen in Fig. 2a)]. The question now is: what is the origin of such peaks? Why are there special values of γ where the motion is more chaotic?
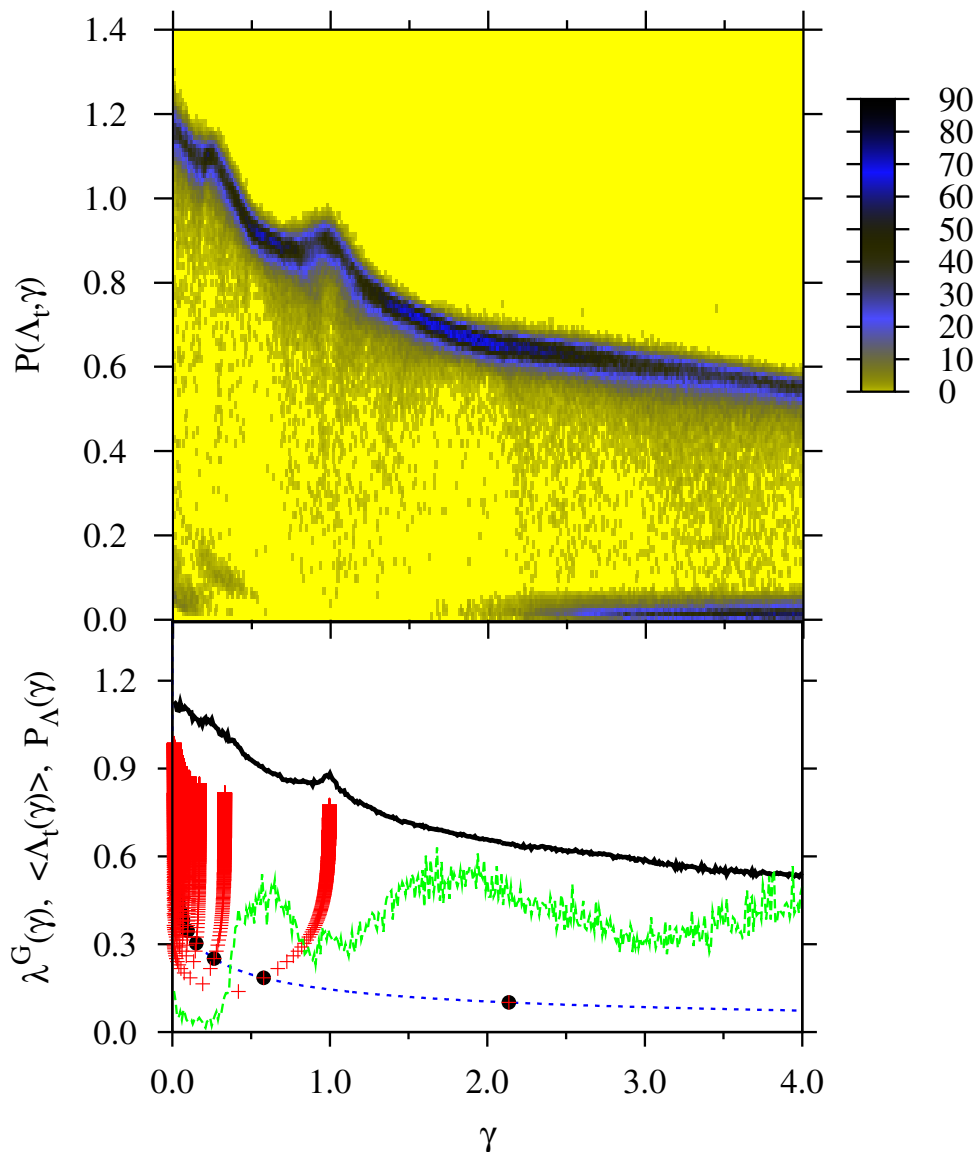

Fig. 2. a)Finite-time distribution of the largest Lyapunov exponent $P(\Lambda_t, \gamma)$ calculated over 400 trajectories up to time $t = 10^4$ and for $r_0 \to \infty$. With increasing $P(\Lambda_t, \gamma)$ the color changes from light to dark (white over yellow and blue to black) and b) mean Lyapunov exponent (solid black line), normalized distribution $P_\Lambda(\gamma)$ of the most probable Lyapunov exponent Λ_t^p (solid gray line) and results for the LE from the Gauss map from Fig. 1.

8

Figure 2(b) also shows the results for the γ dependence of the LE from the Gauss map showed in Fig. 1. We used relations $\theta = \pi x$ and $\gamma(x) = \frac{1-\cos \pi x}{1+\cos \pi x}$ from Eq. (1) to calculate the correspondence between γ and x from the Gauss map. Note that in this interval of γ only the Golden mean point $\overline{1}$ remains from the first sequence (on the right) from Fig. 1. All other points from this sequence have $\gamma > 4.0$. First observation is that the main qualitative behavior of the LE from our physical model follows the curve calculated for the first iteration from the Gauss map (see dashed line). In other words, the main qualitative behavior of the mean LE from the 1D-box with YI follows the period-1 POGM. Second observation is that the pronounced peak observed at $\gamma \sim 1.0$ is *very close* to the point $\gamma(x = \overline{2,800} \sim 1/2)$ which is a period-2 orbit from the Gauss map. We have to remember that this point is very close to the non-periodic orbit $x = 1/2$ from the Gauss map where the LE cannot be calculated. The other pronounced (lower) peak at $\gamma \sim 0.17$ is close to the period-2 orbit $\gamma(x = \overline{4,800} \sim 1/4)$ from the Gauss map. As the value of γ decreases, the LE from the 1D-box with YI follows all peaks obtained from the POGM $x(\gamma) = \overline{k,800}$ $(k = 2, 3, \ldots, 800)$. The important point is, the LE from our physical model follows the behavior of the LE from the LM zero POGM. Therefore, both pronounced peaks at $\gamma \sim 1.0, 0.17$ are probably related to signatures from the *periodic orbits of the HPC*, for which the LE cannot be estimated using the Gauss map.

Another interesting feature appears if we calculate the change of the width of $P(\Lambda_t, \gamma)$ around the most probable Λ_t^p defined through

$$\left. \frac{\partial P(\Lambda_t, \gamma)}{\partial \Lambda_t} \right|_{\Lambda_t = \Lambda_t^p} = 0. \tag{6}$$

This quantity, called $P_\Lambda(\gamma)$, has been proposed [18] as a sensitive measure of 'stickness' in phase-space which are a consequence of the existence of regular islands. Each time this quantity has a minimum, the mixed phase-space of a system is expected to have more trapped trajectories. Otherwise it has an "ergodic-like" motion, then mostly all initial conditions converge to the same finite time LE. For more details about this quantity, some examples and motivations, we refer the readers to [18]. This quantity is plotted in Fig. 2(b) (see gray curve with strong variations). Clearly three minima are observed close to $\gamma \sim 0.25, 1.0, 3.0$ where the dynamics in phase-space has more trapped ('sticky') trajectories. As shown in another work [18], the values $\gamma \sim 1.0, 3.0$ can be related to the integrable cases (genus $g = 1$, see Table 1) from the HPC case. Here we show additional results for mass ratio in the interval $(0.0, 1.0)$. Besides for $\gamma = 3.0$, it is very interesting to observe that $P_\Lambda(\gamma)$ has a minimum for all points for which $\gamma(x = \overline{k,800})$ $(k = 2, 3, \ldots, 800)$ from the Gauss map. As a consequence, $P_\Lambda(\gamma)$ has a minimum in the extended interval $\gamma \sim (0.0, 0.4)$, where these points come closer and closer. Since the points $\gamma(x = \overline{k,800})$ $(k = 2, 3, \ldots, 800)$ are very close to the non-POGM (which are

the PO from the model), it suggest that the minimum of $P_\Lambda(\gamma)$ are due the trapped trajectories reminiscent from the PO from the physical model (with HPC or YI).

Above results allow us to make some statements about the stability of the linear unstable dynamics from the HPC case, i. e., the stability from the different topological surfaces present in the HPC case. Table 1 gives some examples of the relation between the values of $x = \theta/\pi$ with the LE $\lambda^G(x_{k,800})$ from the Gauss map calculated *very* close (on the left) to these points. For example, $\theta/\pi = 1/2(\gamma = 1)$ is an integrable case from the HPC problem with genus $g = 1$ (torus). The LE for the POGM calculated at $\gamma(x = \overline{[2,800]})$ gives $\lambda^G(x_{2,800}) \sim 7.37$. We are proposing that this value of the LE gives a possible "degree of instability" of the torus with genus $g = 1$. We observe in Table 1 that as we increase g, the corresponding values of $\lambda^G(x_{k,800})$ also increase and γ decreases. Therefore, we expect that for higher values of g the invariant surfaces from the HPC case are more unstable. This is verified for the problem considered in this paper (see Fig. 2), where the mean LE increases as the genus g increases following values from Table 1.

5   Conclusions

While the KAM theorem [11] makes some statements about the existence of non-periodic orbits (KAM curves), the residue criterion [13] establishes a correspondence between the existence of a KAM curve and the stability of the periodic orbits that approximate it. Such criterion can be used to determine for which parameter of the model the KAM curves may be destroyed. Here the stability of *periodic orbits with LM zero* from the Gauss map (i. e., the *non-periodic curves* from the physical model) allows us to get some insight about the stability of ISs (no KAM curves) from a linear unstable system with LE *zero* . The linear unstable system considered here is the 1D-box with two particles interacting via HPC. The stability of the IS is obtained by calculating the LE (via Gauss map) from the CF representation of the masses ratio. By perturbing the IS with a Yukawa interaction between particles, we observe that the LEs follow qualitatively the LEs from the Gauss map [see Fig. 2b)]. Only periodic orbits with LM zero from the Gauss map seems to be relevant. Additionally, the two more pronounced peaks in the mean LE [see Fig. 2a)-b)] at $\gamma \sim 1.0$ and ~ 0.17 are explained with results from the Gauss map. They are probably related to signatures from the *periodic orbits of the HPC* case, for which the LE cannot be estimated via Gauss map. This shows a nice example of the relation between the "instability" of a simple CF representation of a number to the LEs from a physical model. We also show that pseudo-integrable systems, where the IS has a higher genus g, are more unstable under perturbations. This is easy to see from Table 1 and Fig. 2b).

As the value of g increases, the corresponding value of γ decreases and the LE increases. Moreless, we were able to show that 'stickness' effects are present each time the mass ratio γ is close to POGM and therefore, close to the nonperiodic orbits from the 1D box with HPC. This was quantified by calculating $P_\Lambda(\gamma)$, which is a sensitive measure of trapped trajectories in phase-space. Each time $P_\Lambda(\gamma)$ has a minimum [see gray line in Fig. 2b)], trapped trajectories in phase-space are expected .

Acknowledgments

References

[1] Mañé R. Ergodic Theory and Differentiable Dynamics. Berlin: Springer Verlag; 1998.

[2] Corless RM, Frank GW, Monroe JG. Chaos and Continued Fractions. Physica D 1990; 46:241-53.

[3] Corless RM. Continued Fractions and Chaos. Am Math Mont 1992; 99:203-15.

[4] Jones WB, Thron WJ. Continued Fractions: Analytic Theory and Applications. Addison-Wesley; 1980); Kim Sh, Ostlund S. Renormalization of Mappings of the 2-Torus. Phys Rev Lett 1985; 55:1165-68.

[5] Fuchss K, Wurm A, Apte A, Morrison PJ. Breakup of shearless meanders and "outer" tori in the standard nontwist map. Chaos 2006; 16: 033120-11.

[6] del-Castillo-Negrete D, Greene JM and Morrison PJ. Renormalization and transition to chaos in area preserving nontwist maps. Physica D 1997; 100:311-29.

[7] Petschel G, Geisel T. Bloch-electrons in Magnetic-fields - Classical Chaos and Hofstadter Butterfly. Phys Rev Lett 1993; 71:239-42.

[8] El Naschie MS. A review of E infinity theory and the mass spectrum of high energy particle physics. Chaos, Solitons and Fractals 2004; 19:209-; El Naschie MS. VAK, vacuum fluctuation and the mass spectrum of high energy particle physics. Chaos, Solitons and Fractals 2003; 17:797-807

[9] Tanaka Y. The mass spectrum of hevaier hadrons and E-infinity theory. Chaos, Solitons and Fractals 2007; 32:996-1007; Tanaka Y. Elementary particle mass, subquark model and E-infinity theory. Chaos, Solitons and Fractals 2006; 28:290-305; Tanaka Y. The mass spectrum of hadrons and E-infinity theory. Chaos, Solitons and Fractals 2006; 27:851-63; Marek-Crnjac L. Chaos, Solitons and Fractals 25 (2005) 807; Tanaka Y. Space-time symmetry, chaos and E infinity theory. Chaos, Solitons and Fractals 2005; 23:335-49.

[10] Paramio M, Sesma J. Invariant Directions in the Henon map. Phys Lett A 1988; 132:98-100.

[11] Lichtenberg AJ, Lieberman MA. Regular and Chaotic Dynamics. Berlin: Springer Verlag; 1992.

[12] del-Castillo-Negrete D, Greene JM, Morrison PJ. Area preserving nontwist maps: Periodic orbits and transition to chaos. Physica D 1996; 91:1-23.

[13] Greene JM. J Math Phys 1979; 20:1183

[14] Satija II. Universal Strange Attractor underlying Hamiltonian Stochasticity. Phys Rev Lett 1987;58:623-26; Farmer JD. Renormalization of the Quasiperiodic transition to Chaos for arbitrary winding numbers. Satija II. Phys Rev A 1985; 31:3520-22.

[15] Richens PJ, Berry MV. Pseudointegrable systems in classical and Quantum-Mechanics. Physica 1981; 2D:495-512.

[16] Gorin T. Generic spectral properties of right triangle billiards. J Math Phys 2001; 34:8281-95.

[17] Gutkin E. Billiards in Polygons. Physica 1986; 19D: 311-33; Gutkin E. Billiards in polygons: Survey of recent results. J Stat Phys 1996; 83:7-26.

[18] Beims MW, Manchein C, Rost JM. Origin of chaos in soft interactions and signatures of non-ergodicity. Submitted.

[19] Glashow SL, Mittag L. Three rods on a ring and the triangular billiard. J Stat Phys 1997; 87:937-41; Cox SG, Ackland GJ. How efficiently do three pointlike particles sample phase space? Phys Rev Lett 2000; 84:2362-2365.

[20] Casati G, Prosen T. Mixing property of triangular billiards. Phys Rev Lett 1999; 83:4729-32.

[21] Kornfeld P, Fomin SV, Sinai YG. Ergodic Theory. Berlin: Springer Verlag; 1982; Walker J. The flying circus of Physics. New York: Wiley;1977; Redner S. A billiard-theoretic approach to elementary one-dimensional elastic collisions. Am J Phys 2004; 72: 1492-98.

[22] Casati G, Ford J. Computer study of ergodicity and mixing in a 2-particle hard points gas system. J Comp Phys 1976; 20: 97-109.

[23] Van Vessen M, Santos MC, Bin Kang Cheng, da Luz MGE. Origin of quantum chaos for two particles interacting by short-range potentials. Phys Rev E 2001; 64: 026201; Miltenburg AG, Ruijgrok ThW. Quantum aspects of triangular billiards. Physica A 1994; 210: 470-88. Koslov VV, Treshchnev DV. Billiards. A Genetic Introduction to the Dynamics of Systems with Impacts. Provindence: American Mathematical Society; 1991.

[24] Shudo A, Shimizu Y. Extensive numercial study of spectral statistics for rational and irrational polygonal billiards. Phys Rev E 1993; 47: 54-62.

[25] Arnold VI, Avez A. Ergodic Problems of Classical Mechanics. New-York: Benjamin; 1968.

[26] Cipriani P, Denisov S, Politi A. From anomalous energy diffusion to levy walks and heat conductivity in one-dimensional systems. Phys Rev Lett 2005; 94: 244301; Grassberger P, Nadler W, Yang L. Heat conduction and entropy production in a one-dimensional hard-particle gas Phys Rev Lett 2002; 89: 180601.

[27] Meza-Montes L, Ulloa SE. Dynamics of two interacting particles in classical billiards. Phys Rev E 1997; 55: R6319-22.

[28] Crisanti A, Paladin G, Vulpiani A. Products of random matrices in Statistical Physics.Heidelberg: Springer-Verlag; 1993; Sepúlveda MA, Badii R, Pollak E. Spectral-analysis of conservative dynamical-systems. Phys Rev Lett 1989; 63: 1226-29.